Earth and Planetary Science Letters 305 (2011) 1–10

Contents lists available at ScienceDirect

Earth and Planetary Science Letters

journal homepage: www.elsevier.com/locate/epsl

Chondrites as samples of differentiated planetesimals

Linda T. Elkins-Tanton *, Benjamin P. Weiss, Maria T. Zuber

Department of Earth, Atmospheric, and Planetary Sciences, Massachusetts Institute of Technology, Cambridge, MA, USA

ARTICLE INFO

Article history:
Received 30 June 2010
Received in revised form 2 March 2011
Accepted 9 March 2011

Editor: T. Spohn

Keywords:
Chondrite
planetesimal
magma ocean
differentiation
Allende

ABSTRACT

Chondritic meteorites are unmelted and variably metamorphosed aggregates of the earliest solids of the solar system. The variety of metamorphic textures in chondrites motivated the "onion shell" model in which chondrites originated at varying depths within a parent body heated primarily by the short-lived radioisotope ^{26}Al, with the highest metamorphic grade originating nearest the center. Allende and a few other chondrites possess a unidirectional magnetization that can be best explained by a core dynamo on their parent body, indicating internal melting and differentiation. Here we show that a parent body that accreted to >~200 km in radius by ~1.5 Ma after the formation of calcium–aluminum-rich inclusions (CAIs) would have a differentiated interior, and ongoing accretion would add a solid undifferentiated crust overlying a differentiated interior, consistent with formational and evolutionary constraints inferred for the CV parent body. This body could have produced a magnetic field lasting more than 10 Ma. This hypothesis represents a new model for the origin of some chondrites, presenting them as the unprocessed crusts of internally differentiated early planetesimals. Such bodies may exist in the asteroid belt today; the shapes and masses of the two largest asteroids, 1 Ceres and 2 Pallas, can be consistent with differentiated interiors, conceivably with small iron cores with hydrated silicate or ice–silicate mantles, covered with undifferentiated crusts.

1. Introduction

The antiquity and abundance of CAIs in CV chondrites have long suggested an early parent body accretion age. New Pb–Pb and Al–Mg ages of chondrules in CVs indicate that they may be among the oldest known in any chondrite class, with ages ranging from ~0 to ~3 Ma after CAIs (Amelin and Krot, 2007; Connelly et al., 2008; Hutcheon et al., 2009) (Fig. 1). The time of accretion of a body controls the amount of initial ^{26}Al, which was likely uniformly distributed in the inner protoplanetary disk (Jacobsen et al., 2008). Bodies that accreted to more than ~20 km radius before ~1.5 Ma after the formation of CAIs likely contained sufficient ^{26}Al to melt internally from radiogenic heating (Hevey and Sanders, 2006; Merk et al., 2002; Sahijpal et al., 2007; Urey, 1955). These early-accreting bodies would have melted from the interior outward, resulting in an interior magma ocean under a solid, conductive, undifferentiated shell (Ghosh and McSween Jr., 1998; Hevey and Sanders, 2006; McCoy et al., 2006; Merk et al., 2002; Sahijpal et al., 2007; Schölling and Breuer, 2009). This shell would consist of the same chondritic material that made up the bulk accreting body before melting began; further, and critically, ongoing accretion would add undifferentiated material to the crust, and this material may even have bulk compositions distinct from the differentiated interior.

Allende and a few other chondrites possess a unidirectional magnetization (Butler et al., 1972; Nagata and Funaki 1983; Carporzen et al., 2010; Weiss et al., 2010). Funaki and Wasilewski (1999) suggested a liquid metallic core dynamo origin for magnetism on the CV parent body. Carporzen et al. (2010) described how unidirectional magnetization in Allende is consistent with a field lasting >10 Ma. The variety of metamorphic textures in chondrites originally motivated the "onion shell" model in which chondrites originated at varying depths within a parent body heated primarily by the short-lived radioisotope ^{26}Al, with the highest metamorphic grade originating nearest the center (Miyamoto et al., 1981; Taylor et al., 1987). Now, the metamorphic, magnetic, and exposure age data collectively indicate a new model for the CV chondrite parent body in which interior melting is incomplete and a magma ocean remains capped by an undifferentiated chondritic shell. This conductive lid insulates the internal magma ocean, slowing its cooling and solidification by orders of magnitude while still allowing sufficient heat flux out of the core to produce a dynamo with intensities consistent with magnetization in Allende [see analysis in Weiss et al. (2008, 2010)]. Materials in the undifferentiated lid experienced varying metamorphic conditions.

Chondritic meteorite samples, including Allende, provide motivation for this study. We seek to define the accretion age and size that would allow internal differentiation of a body consistent with Allende originating in the unmelted crust. A chondritic surface, a silicate or

* Corresponding author at: Department of Earth, Atmospheric, and Planetary Sciences, Massachusetts Institute of Technology, Cambridge, MA 02139, USA. Tel.: +1 617 253 1902.
E-mail addresses: ltelkins@mit.edu (L.T. Elkins-Tanton), bpweiss@mit.edu (B.P. Weiss), zuber@mit.edu (M.T. Zuber).

0012-821X/$ – see front matter © 2011 Elsevier B.V. All rights reserved.
doi:10.1016/j.epsl.2011.03.010

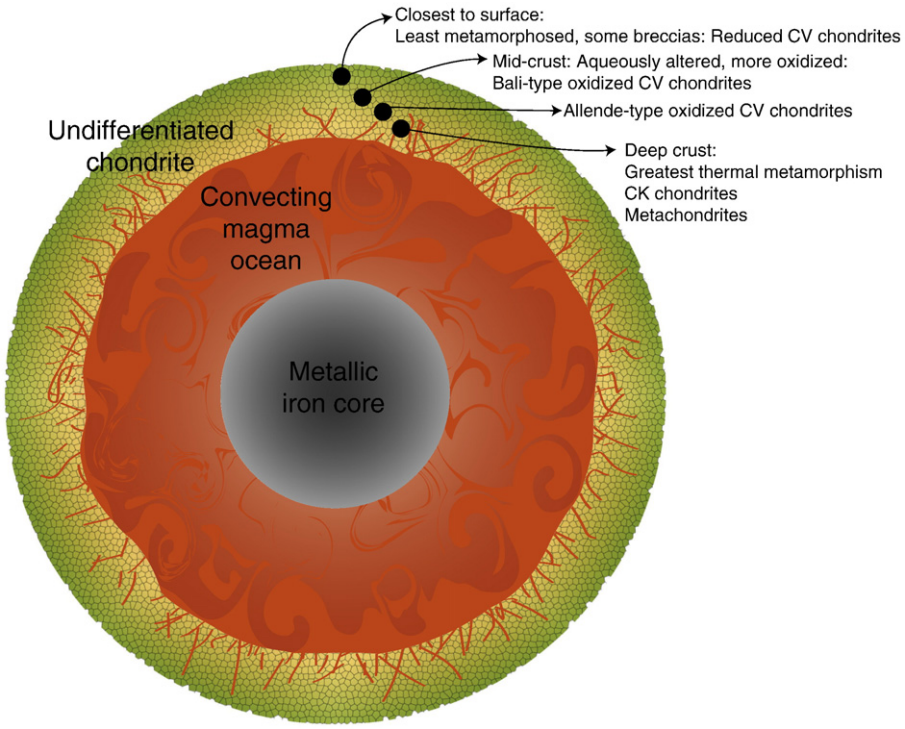

Fig. 1. Schematic diagram of proposed structure for the CV parent body, including an iron core, internal magma ocean, and undifferentiated chondritic crust with varying levels of metamorphism and metasomatism.

ice–silicate mantle and crust, and an iron core should characterize such a body. Further, we will investigate the implications of internally differentiated bodies, including their possible existence in the asteroid belt today. This study is designed to test the feasibility of internal differentiation with a retained primitive crust, and the feasibility of generating a long-lived magnetic core dynamo on such a body.

2. Models and methods

To calculate heat fluxes, the possibility of a core dynamo, and temperature gradients in the unmelted crust, we assume instantaneous accretion and solve the heat conduction in a sphere with initial ^{26}Al evenly distributed (Hevey and Sanders, 2006). The body is heated homogeneously but radiates energy into space, producing a hot interior and chilled crust. If the interior exceeds its solidus temperature sufficiently, the resulting interior magma ocean would advect heat to the base of the crust, where heat transfer continues through the far slower process of conduction.

Although new models and observations indicate rapid accretion (Johansen et al., 2007), the accretion of planetesimals early in solar system history was certainly not instantaneous, as discussed in Ghosh et al. (2003), Merk et al. (2002), and Sahijpal et al. (2007). The heat of accretion during incremental accretion may be neglected here; it does not significantly change the thermal results of these models. A hypothetical parent body with 300-km radius receives ~10^{25}J in kinetic energy during incremental accretion, sufficient to heat the body homogeneously by only 10 to 20 °C (see SD). Thus the first-order temperature driver prior to 2 Ma after CAIs was ^{26}Al heating. The complexity and stochastic nature of boundary conditions, sizes and rates of impactors, and energy partitioning during incremental accretion also mean that incremental model results are necessarily non-unique. Incremental accretion models are likely therefore to require a Monte Carlo approach. Because our intention is to demonstrate the feasibility of partial differentiation rather to model it explicitly, we conclude that instantaneous accretion is a reasonable simplification for calculating core heat flux.

Incremental accretion, though it may not influence the heating of the body, does strongly influence cooling. A thickening conductive undifferentiated lid added to an initially partially melted planetesimal will slow its heat flux into space and therefore lessen the driving mechanism for a magnetic core dynamo, while lengthening its duration. A simple model of incremental accretion is considered in comparison to the instantaneous models; this model is described below.

2.1. Heating and heat transfer

The initial ^{26}Al content of CV chondrites is a controlling parameter in these calculations. Kunihiro et al. (2004) find that there is insufficient radiogenic aluminum in CO chondrites to cause more than minimal melting even with the help of radiogenic ^{60}Fe, and also argue that the CV parent body was unlikely to have melted. However, their conclusion for CV chondrites is based on an initial ^{26}Al content identical to that of CO chondrites and instantaneous accretion. Here we find that the potentially older age of CV chondrules (the youngest being up to 1 Ma older than those in CO chondrites) combined with non-instantaneous accretion mean the CV body could have melted. See Table 1 for model parameters including bulk aluminum content.

Following Hevey and Sanders (2006) we begin by assuming instantaneous accretion and solve the heat conduction in a sphere with initial ^{26}Al evenly distributed:

$$\rho C_P \frac{\partial T}{\partial t} = \frac{1}{r^2}\frac{\partial}{\partial r}\left(kr^2\frac{\partial T}{\partial r}\right) + A_0(r,t), \quad (1)$$

where ρ is density, C_P is the heat capacity of the chondrite, T is temperature, t is time, r is radius, k is thermal conductivity, and A_0 is the radiogenic heat source per volume per time. The temperature

Table 1
Parameters used in models.

Variable	Symbol	Value(s)	Units	Ref.
Initial and surface temperature	T_0	250	K	Woolum and Cassen (1999)
Planetesimal radius	r	50,000, 100,000, 200,000, 300,000, 400,000, 500,000	m	
Age of instantaneous accretion		0, 1, 1.5	Ma after CAI formation	
Metal in bulk starting material (for core formation)		0.05, 0.1, 0.2	Volume fraction	
Density of conductive lid	$\rho_{\_LID}$	2900	kg m^{-3}	Britt and Consolmagno (2003)
Density of planetesimal magma ocean	$\rho_{\_MO}$	3000	kg m^{-3}	
Density of iron core	$\rho_{\_CORE}$	8000	kg m^{-3}	
Thermal diffusivity of crust	κ	8×10^{-7}	m^2 s^{-1}	Opeil et al. (2010)
Thermal diffusivity of core	κ	6×10^{-5}	m^2 s^{-1}	Monaghan and Quested (2001)
Thermal conductivity of conductive lid	K_{LID}	1.5	W m^{-1} K^{-1}	Opeil et al. (2010)
Thermal conductivity	K	2.1	W m^{-1} K^{-1}	
Heat capacity of silicates	C_P	800	J kg^{-1} K^{-1}	Fabrichnaya (1999), Ghosh and McSween Jr. (1999)
Heat capacity of iron core	C_{P_CORE}	850	J kg^{-1} K^{-1}	Bartels and Grove (1991)
Heat of fusion of silicates	H_f	400,000	J kg^{-1}	Ghosh and McSween Jr. (1998)
Heating production of ^{26}Al decay	H_0	0.355	W kg^{26}Al^{-1}	Castillo-Rogez et al. (2009)
Aluminum content of CV chondrites	X_{Al}	1.8	wt%	Lodders and Fegley (1998)
Initial ^{26}Al/^{27}Al ratio	$^{26}Al_0$	5×10^{-5}		Lee et al. (1976), MacPherson et al. (1995)
Fraction of ^{26}Al in bulk material	C	$^{26}Al_0\, X_{Al}$		
Decay constant	λ	3.0124×10^{-14}	s^{-1}	Castillo-Rogez et al. (2009)

profile in these planetesimal models is initially calculated using an analytic solution as given by Carslaw and Jäger (1946) and Hevey and Sanders (2006):

$$T = T_0 + \frac{\kappa A_0}{K\lambda} e^{-\lambda t}\left|\frac{R\sin\left(r\left(\frac{\lambda}{\kappa}\right)^{\frac{1}{2}}\right)}{r\sin\left(R\left(\frac{\lambda}{\kappa}\right)^{\frac{1}{2}}\right)} - 1\right| + \frac{2R^3 A_0}{r\pi^3 K}\sum_{n=1}^{\infty}\frac{-1^n}{n\left(n^2 - \frac{\lambda R^2}{\kappa\pi^2}\right)}\sin\left(\frac{n\pi r}{R}\right)e^{-\frac{\kappa\pi^2 n^2 t}{R^2}} \quad (2)$$

where the variables are as defined in Table 1, and t is the time elapsed since accretion. The power from ^{26}Al, A_0 in W m^{-3}, is obtained by multiplying the decay energy of aluminum, converted to J kg^{-1}, with the aluminum content of chondrites, the ^{26}Al decay constant, the material density, and the initial ^{26}Al/^{27}Al ratio, and similarly for the other radioactive nuclides considered (see Supplementary Data, SD). To obtain the initial power for later accretion times, the initial A_0 is multiplied by $e^{-\lambda t}$, where t is here the instantaneous time of accretion.

The accreted chondritic material is assumed to begin to melt at 1200 °C and reach its liquidus at 1600 °C at the low but non-zero pressures of the planetesimal interiors (in a Vesta-sized body the pressure at the bottom of a mantle magma ocean will be 1 kb or less, and over that pressure range the solidus will change by less than 20 °C and the adiabat by less than 4 °C). These temperatures are based on experimental melting of Allende bulk compositions (Agee et al., 1995) taking into consideration the absence of the iron metal component (removed to the core) and the loss of some volatiles. Melting is calculated using the following simplified expression for melt production per degree above the solidus:

$$f = \Delta T\frac{df}{dT} = \Delta T\frac{C_P}{H_f} = (0.002)\Delta T \quad \text{[fraction by weight]}, \quad (3)$$

where C_p and H_f are the heat capacity and heat of fusion of the silicates, and ΔT is the temperature excess of the melt source beyond its solidus (Hess, 1992). The coefficient 0.002 therefore has units of K^{-1} and the resulting f is a nondimensional weight fraction.

Latent heat of melting is similarly applied to the temperature of the melting material. The total temperature change for complete melting in this simple linear melting scheme, using values from Table 1, is

$$T = \frac{H_f}{C_P} \approx 500K. \quad (4)$$

The latent heat temperature change is applied to the melting material at each time step of the model until complete melting is achieved. The model tolerates temperatures in the magma ocean above the liquidus temperature, and conductive heat loss through the lid continues. High temperatures lead to melting and thus thinning of the lid.

We calculate thermal profiles using Eq. (2) at intervals of 1000 years until the body has melted 10% by volume (so much radiogenic heat is created in these bodies that the degree of melting is 100%, and volume here refers to a fraction of the total planetesimal volume). After this point, the internal magma ocean is treated as a homogeneous adiabatic fluid, and conduction of heat through the unmelted crust limits the heat flux available to drive the core dynamo.

These calculations are done using a finite difference formulation of the heat conduction equation in spherical coordinates for the conductive lid, which is defined as the material at temperatures below 1400 °C based on an assumption that melting above 50% will produce a convecting fluid no longer constrained by a solid network of residual crystals. In this simulation all material in the conductive lid is assumed to be porous, unmelted chondritic material. Although the temperature profiles indicate areas of partial melt and sintering, these are not treated in the calculations.

At each step the heating contributions of ^{235}U, ^{238}U, ^{232}Th, ^{40}K, and ^{26}Al are added, assuming chondritic concentrations, to each element in the conductive lid and to the bulk magma ocean beneath. Concentrations, heat production, and calculation schema for U, Th, and K are from Turcotte and Schubert (2002); Al values and references are listed in Table 1. Heating from ^{26}Al is given by

$$H(t) = H_0 C_0 e^{-\lambda t}\left[\text{W kg}^{-1}\right], \quad (5)$$

where H_0 is heating rate of ^{26}Al, C_0 is the fraction of ^{26}Al in the bulk material, and λ is the decay constant for ^{26}Al. For values and references see Table 1.

Radiogenic heat is added to the crust in proportion to the silicate portion of the bulk chondrite, subtracting volume for pore space,

assumed to be 25%, and for metal fraction, and to the magma ocean, which is assumed to be 100% bulk silicate.

Heat is conducted upward from the magma ocean to the surface through the conductive lid using the following expression for temperature controlled by heat conduction in a sphere:

$$T_r^t = T_r^{t-dt} + \kappa dt\left(\frac{1}{r}dr\left(T_{r+dr}^{t-dt} - T_{r-dr}^{t-dt}\right) + \frac{1}{dr^2}\left(T_{r+dr}^{t-dt} - 2T_r^{t-dt} + T_{r-dr}^{t-dt}\right)\right) + dt\frac{H}{C_P}, \quad (6)$$

where dt is a Courant time step determined by thermal diffusivity, and dr is the radial length of an element in the finite difference grid that does not exceed 1 km. At each time step the temperature at the bottom of the conductive lid is examined, and if the bottom of the lid has melted, the radius of the bottom of the grid is adjusted upward and the grid points redefined; latent heat is also considered at each melting step. If more melting has occurred then the appropriate volume is added to the core, at the current temperature of the magma ocean.

Although iron–nickel metal melts at temperatures below primitive silicate melting temperatures, the metal liquid may be unable to segregate into a core until the silicates are partially molten. Previous studies differ on whether core segregation occurs near 950 °C, at the iron alloy eutectic, or in the range 1170 to 1570 °C, between the solidus and liquidus of the silicate portion [see Sahijpal et al. (2007) and references therein]. Here we assume metallic core formation occurs instantaneously when the bulk chondritic material reaches its model solidus, 1200 °C. At the point that the body has reached 10% melting by volume, the core is assumed to be at thermal equilibrium with the small internal magma ocean from which it just segregated (for a 100-km radius body, at 10 vol.% melting the internal convecting magma ocean reaches a radius of about 46 km, and if the body began with 20 vol.% metals the core has a radius of 30 km).

The core is assumed to contain no U, Th, K, or Al; all these elements are compatible with the silicate magma ocean and not with the metallic core material. Thus the core, initially at thermal equilibrium with the overlying magma ocean, has a thermal history entirely driven first by the radiogenic heating of the overlying magma ocean (during which the core is heated by the magma ocean, and heat flux is therefore into rather than out of the core), and then by secular cooling of the body (during which the core cools and heat moves back into the magma ocean).

To calculate these changes, at each time step heat flux through the core–mantle boundary is calculated as

$$F_{core} = \kappa_{core}\rho_{core}C_{p,core}\frac{dT}{dr}\left[\mathrm{J\ m^{-2}\ s^{-1}}\right], \quad (7)$$

and the resulting temperature change in the core is given as

$$\Delta T_{core} = \frac{3dtF_{core}}{P_{core}C_{P,core}r_{core}}\ [\mathrm{K}], \quad (8)$$

which is a simplification in this geometry of the general statement

$$\Delta T = \frac{dtF_{core}A_{core\_surface}}{V_{core}\rho_{core}C_{p,core}}. \quad (9)$$

The corresponding temperature change in the magma ocean is given as

$$\Delta T_{MO} = \frac{3dtF_{core}r_{MO,top}^2}{\rho_{MO}C_{P,MO}\left(r_{MO,top}^3 - r_{core}^3\right)}\ [\mathrm{K}], \quad (10)$$

where $r_{\mathrm{MO,top}}$ is the radius at the top of the internal magma ocean, equivalent to the radius at the bottom of the conductive lid. Next, the heat flux out of the magma ocean and into the conductive lid is calculated using an equivalent statement to Eq. (6), and the corresponding additional temperature change in the magma ocean is calculated using an equivalent statement to Eq. (9).

The physics and chemistry of cooling an internal magma ocean on a small body are not well understood. Mineral phases solidifying from the magma ocean will be dense in comparison to the magma ocean, with the exception of plagioclase feldspar. The time required for mineral grains to either sink or float out of the convecting magma ocean is, however, possibly longer than the time of solidification of the body (Elkins Tanton et al., 2008). We therefore assume for simplicity that the conductive lid does not significantly thicken from beneath while the internal magma ocean is still convecting, as that would require material to adhere to its bottom and leave the convecting magma ocean. Rather, the magma ocean continues to convect and cool and fractionate under the existing thinnest conductive lid. Convection is assumed to be inhibited at temperatures below 1000 °C by a high crystal fraction in liquids evolved through some degree of fractional solidification. No latent heat of solidification is applied during cooling.

For the simple incremental accretion model shown here, the initial assumptions are the same: A radius of instantaneous accretion is chosen and heating calculated until 10% of the planetesimal's volume is melted. The calculations are then passed to the convective code, with conduction occurring through the unmelted lid. Shells of cold undifferentiated material are added to the outside of the planetesimal in increments of equal radius until a final radius is acquired, in a simple approximation of the addition of new material to the outside of the planetesimal. Thus, heat flux is inhibited through the growing lid. The new material added to the exterior is assumed to have the same radioactive element composition as the initial material.

2.2. Calculating internal structure in asteroids

To address whether examples of differentiated parent bodies of the kind we propose are conceivably preserved in the asteroid belt today, we consider the simple case of a rotating, hydrostatic figure composed of a core and mantle, each of uniform density (Fig. SD2). For such a body it is possible to relate shape, gravitational moments and internal structure. We invoke the formalism of Dermott (1979), who derived a relationship between the moment of inertia factor (C/Ma^2) and the internal density structure for a planetary body with this configuration

$$\frac{C}{Ma^2} - \frac{2}{5}\left[\frac{\rho_m}{\langle\rho\rangle} + \left(1 - \frac{\rho_m}{\langle\rho\rangle}\left(\frac{r_c}{R}\right)^2\right)\right], \quad (11)$$

where M, R and $<\rho>$ represent the mass, radius and mean density of the body, C is the moment about the polar axis, a is the semi-major equatorial axis, r_c is the core radius, and ρ_m and ρ_c are the mantle and core densities. Introducing an expression for the mean density

$$\langle\rho\rangle - \frac{\left(\frac{4}{3}\right)\pi\left[\rho_c r_c^3 + \rho_m\left(R^3 - r_c^3\right)\right]}{\left(\frac{4}{3}\right)\pi R^3} \quad (12)$$

allows the mantle and core densities to be expressed as

$$\rho_m - \langle\rho\rangle\left[\frac{\frac{5}{2}\frac{C}{Ma^2} - \left(\frac{r_c}{R}\right)^2}{1 - \left(\frac{r_c}{R}\right)^2}\right], \quad (13)$$

and

$$\rho_C - \frac{\langle\rho\rangle - \rho_m\left[1-\left(\frac{r_C}{R}\right)^3\right]}{\left(\frac{r_C}{R}\right)^3}. \quad (14)$$

The consistency of internal structures with the hydrostatic assumption can also be tested using an expression between hydrostatic flattening and moment of inertia factor (Jeffreys, 1959)

$$f_{hyd} = \frac{q}{1+\left(\frac{25}{4}\right)\left[1-\left(\frac{3}{2}\right)\frac{C}{Ma^2}\right]} \quad (15)$$

where

$$q = \frac{\omega^2 a^3}{GM}, \quad (16)$$

and ω is the rotational angular velocity and G is the universal constant of gravitation.

On the basis of observations of shape, mass and surface composition inferred from infrared spectra, we consider asteroids 1 Ceres and 2 Pallas as the likeliest candidates among the largest asteroids for the proposed parent body and we investigate models of their interior structures using the expressions above. Fig. SD3 plots expression (15) combined with axial measurements in Table SD2, and verifies the validity of the hydrostatic shape of both bodies within the bounds of measurement error.

These simple calculations are intended to demonstrate the plausibility of the present-day existence of a differentiated CV chondrite parent body. Additional observations will be required to test more rigorously whether either or both of these bodies (or others) satisfy all required criteria.

3. Results

If accreted before ~1.5 Ma after CAIs, the planetesimal melts from its interior through radiogenic heat. In the largest body considered here, 500 km radius, an internal magma ocean is still generated if the body accretes by 1.6 Ma after CAIs, but for smaller bodies and at any later accretion times there is insufficient heat to produce an internal magma ocean (Fig. 2). This precise ending point of melting is dependent upon initial parameters that might not be well constrained, including initial ^{26}Al content of the parent body and thermal diffusivity of the variably porous and sintered conductive lid.

Calculation of core heat flux is a necessary first step to determine the possibility of a core dynamo. Here the rapid heat transfer of convection in a liquid internal magma ocean maximizes core heat flux. The magma ocean rapidly heats beyond the temperature of the non-radioactive core, so initial heat flux across the core–mantle boundary transfers heat into the core, rather than out. All bodies considered here reach their peak magma ocean temperatures within 5 Ma after CAI formation (Figs. 3 and 4). Shortly after radiogenic heating peaks and the body begins secular cooling heat flux from the core becomes positive, compatible with creating a core dynamo. (Heat flow into a core may be able to drive a core dynamo, but investigation of this novel and speculative effect is not included in this paper.)

All bodies considered here have sufficient size to produce a core dynamo. Bodies larger than ~100 to 150 km radius will produce a core dynamo lasting longer than 10 Ma, and those larger than ~300 to 350 km radius will produce a core dynamo lasting longer than 50 Ma (Fig. 3). The volume fraction of metal in the bulk material determines the size of the core, but over the range of metal fractions considered here (0.05 to 0.2), core heat flux and thus magnetic dynamo are not greatly affected (Fig. 4).

As shown by Hevey and Sanders (2006), these early-accreting planetesimals melt extensively and retain only a very thin crust. In the instantaneous accretion convective models used here the crust is artificially limited to a thickness no less than 2% of the body's radius (Fig. 5). Only in bodies accreting later than ~1.3 Ma are thicker crusts naturally retained on the bodies; radiogenic heating is lower and so less of the planetesimal's shell melts. The thermal gradient within the stable undifferentiated crust, from liquid silicate temperatures at its bottom boundary to space equilibrium blackbody temperatures at its surface (Hevey and Sanders, 2006; Sahijpal et al., 2007), would produce regions of varying metamorphic grade.

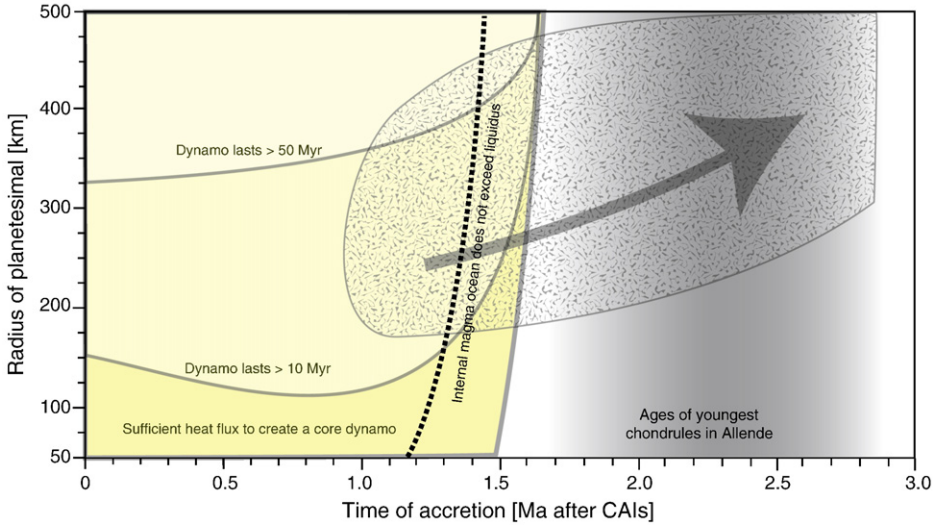

Fig. 2. Summary of model results for the CV chondrite parent body and predictions for its size and thermal history. Bodies with sufficient heat flux to create a core dynamo assuming instantaneous accretion are shown in yellow. Additional contours are given showing the longevity of the resulting core dynamo. The ages of the youngest chondrules in Allende are shown in the vertical grey band. Constraints from Allende indicate that its parent body had a long-lived magnetic field (lasting until at least 10 Ma after CAIs), and a thick unmelted crust. Accretion over a period of time is therefore required. We suggest a path of accretion that lies in the patterned area; the arrow is an example path. Earlier accretion to a given radius produces a body with such a thin crust that foundering is likely. The body must accrete closer to 1 Ma, so that internal temperatures do not rise too high, and then continue accreting material to the crust while the core dynamo continues.

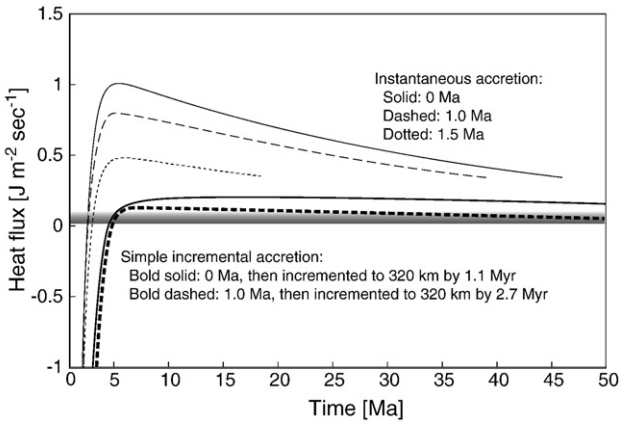

Fig. 3. Core heat flux from planetesimals as a function of time after CAIs formation. Planetesimals with radius 300 km are shown at three ages of instantaneous accretion: 0, 1.0, and 1.5 Ma after CAI formation. Two additional models are shown with instantaneous accretion at 0 and 1.0 Ma after CAIs, followed by regular increments of cold material to the planetesimal surface until the total radius equals 320 km. The shaded region at bottom marks the heat fluxes that must be exceeded for the production of a core dynamo. When internal temperatures fall below 1000 °C convection is assumed to cease and the calculations are terminated.

The simple incremental accretion models, in which the initially instantaneous core then receives increments of cold material to its surface over an additional 1 to 2 Myr, would also produce core dynamos. The thickening cold crust inhibits heat flux out of the body and so lessens core heat flux but also lengthens the period of internal convection (Fig. 3). Determining the combinations of rate of accretion and final body size that allow or disallow magnetic dynamos is beyond the scope of this project, but these initial studies indicate that dynamos can be lengthened by adding insulating crust, and that very thick added crusts would inhibit dynamos.

Asteroid 1 Ceres displays a hydrostatically relaxed shape from which its internal structure has previously been modeled (Castillo-Rogez and McCord, 2010; Thomas et al., 2005). And a recent analysis of the shape of 2 Pallas (Schmidt et al., 2009) finds a close fit of the shape to a hydrostatically relaxed spheroid. Given current knowledge of shape, Ceres is most consistent with a differentiated interior, as

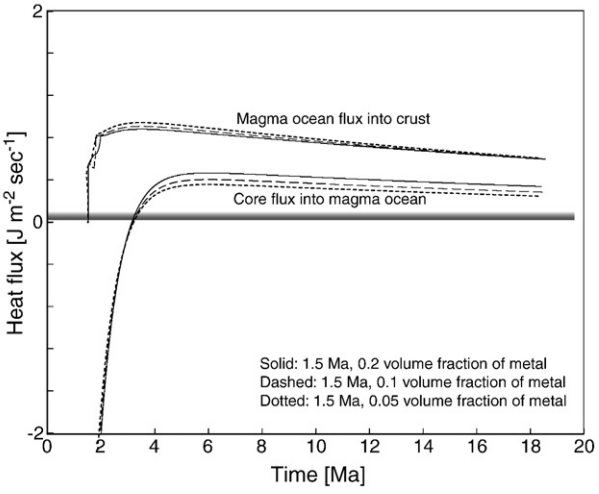

Fig. 4. Magma ocean and core heat fluxes for 300-km-radius bodies accreted instantaneously at 1.5 Ma after CAI formation as a function of the volume fraction of Fe metal in the body. The core heat fluxes are comparable for bulk metal contents of 0.05, 0.1, and 0.2 volume fractions. All bodies melt to within 10 km of the surface. The radii of the final cores produced through metal segregation at every melting increment are 108 km, 137 km, and 172 km, respectively.

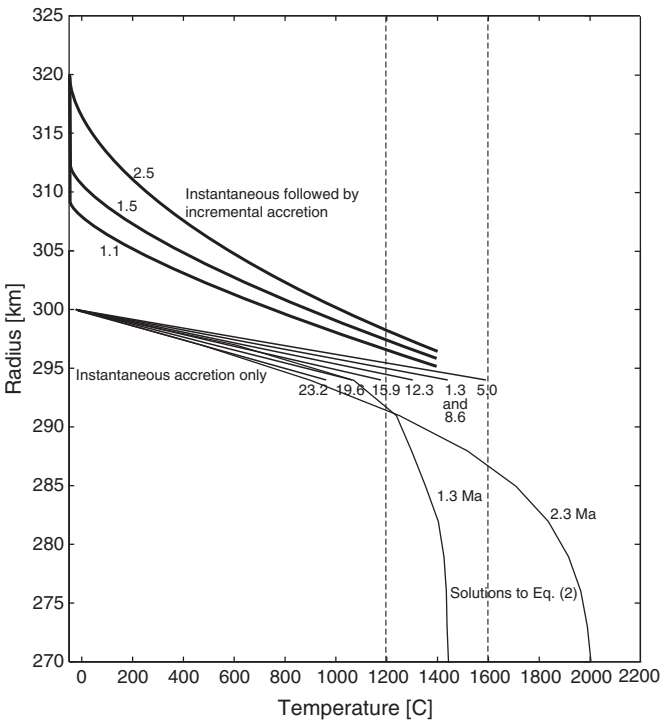

Fig. 5. Temperature profiles in the conductive unmelted lid of a planetesimal that accreted instantaneously at 1.0 Ma after CAIs. Thin lines: profiles in the conductive lid overlying a homogeneously mixed internal magma ocean at the temperature of the bottom of the lid, seven times as labelled. Bold lines: a body that instantaneously accreted, then received regular increments of cold material to the planetesimal surface until the total radius equals 320 km at 1.1 Ma, at three times as labelled. Dashed lines: solidus and liquidus. Two fine lines that extend to depth, from Eq. (2): temperature profile at 1.3 Ma, passed to the convective code, and a later profile at 2.3 Ma, included for comparison. The temperatures at the bottom three nodes of the conductive lid at 5.0 Ma exceed our stated lid temperature of 1400 °C, but the lid is constrained in the code to be no thinner than 2% of the planetesimal radius, or in this case, 6 km. The 6 km limit was reached at 1.3 Ma and retained afterward. Note that the solution to Eq. (2) at 2.3 Ma gives a lid under 1400 °C that is ~10 km thick, rather than the ~6 km thickness from this code; allowing the interior to be convectively well-mixed removes the curving boundary layer.

previously noted (Thomas et al., 2005), but both undifferentiated and differentiated interiors are permissible for Pallas.

An assumed iron core of ρ_c ~7800 kg m^{-3} in 1 Ceres constrains the core to radius to $0.22<r_c/R<0.5$ and limits mantle density to $1000<\rho_m<1950$ kg m^{-3} (Fig. 6). For Pallas, assumption of an iron core, again with density ρ_c-7800 kg m^{-3} yields a range of fractional core size of $0.3<r_c/R<0.6$ and constrains the mantle density to $1000<\rho_m<2300$ kg m^{-3} (Fig. 6). A mantle density of 1000 kg m^{-3} implies pure water ice, while higher values likely indicate mixed ices and silicates.

4. Discussion

4.1. Core dynamos on planetesimals

These core dynamo calculations have several caveats. Heat flux through the undifferentiated crust may be enhanced by fluid flow (Young et al., 2003) or slowed by a porous low-conductivity crust (Haack et al. 1990). If a body 250 km or more in radius accretes as late as ~2.0 Ma after CAIs, its internal temperature reaches ~1000 °C and it may form a core, but its silicate mantle will not melt more than a small fraction; compositional convection in the core would then likely be necessary for dynamo generation (Nimmo, 2009). Therefore, ~2.0 Ma is the latest limit on accretion that will allow a core dynamo using the parameters chosen in these models. The upper time limit is sensitive to choice of heat capacity, final body radius,

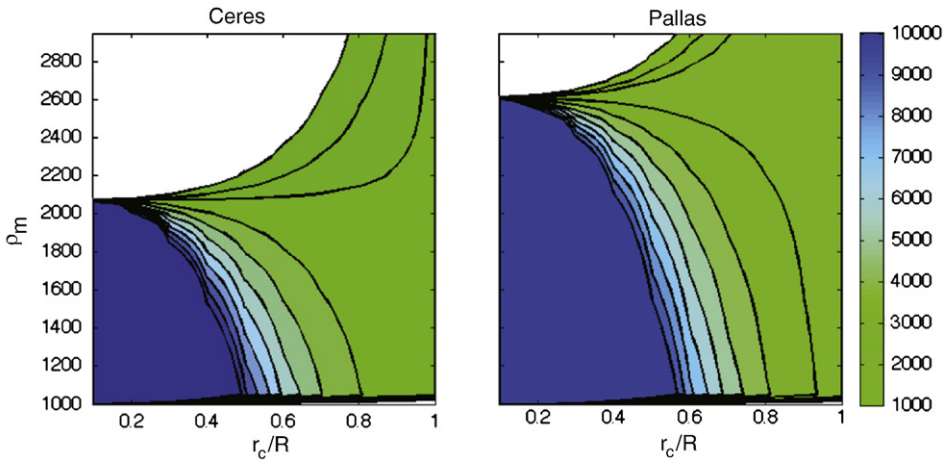

Fig. 6. Contours of core density (ρ_c) for core radius/planetary radius (r_c/R) and mantle density (ρ_m) for 1 Ceres (left) and 2 Pallas (right). Core densities in the range of iron metal but as light as pure silicate are consistent with observations. Both bodies have mantle densities consistent with an ice and silicate mixture.

^{26}Al and ^{60}Fe content, and thermal boundary conditions and has uncertainties of ~±1 Ma.

Throughout most of the parameter space explored here bodies would create dynamos lasting tens of millions of years (Fig. 2), consistent with the paleomagnetic record of Allende (Carprozen et al., 2010). Our code halts calculation when the magma ocean is assumed to end convection, but even conductive heat flux may be sufficient to drive dynamos in some cases. Sufficient heat flux for a core dynamo is a pervasive and robust outcome in these models. Although convection is a necessary but not sufficient criterion for

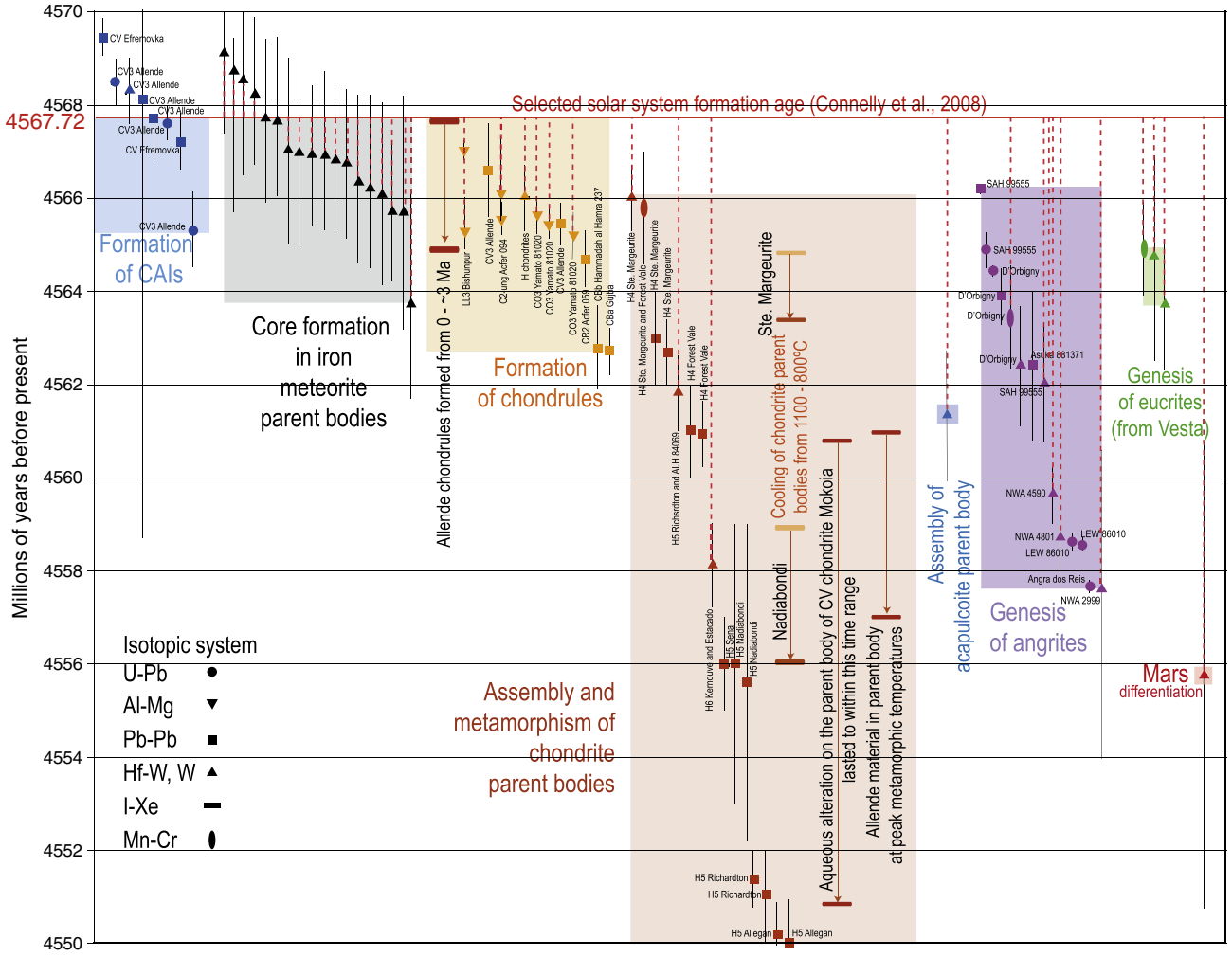

Fig. 7. Age constraints on meteorite and parent body evolution. Red dashed lines indicate ages calculated relative to the selected age of oldest CAI. The early ages of CV chondrite chondrules and CV meteorite evidence for relatively protracted thermal metamorphism indicate an early accretion age for the CV parent body. All dates and references in Table SD1.

dynamo action, it appears feasible that planetesimals also had other properties (core size, core convective velocity, and spin rate) suitable for dynamo generation (Weiss et al., 2008, 2010).

4.2. The crust of a planetesimal

The body must retain or acquire a sufficiently thick crust to both create radial source zones for each chondrite type and to be stable against foundering. Metasomatism of Allende likely began about 5 Ma after CAI formation (Gilmour et al., 2009), as water was mobilized within the planetesimal. The presence of talc and the absence of serpentine indicate peak temperatures of ~300–350 °C (Brearley, 1997; Krot et al., 1995), while organic thermometry and presolar gases in nanodiamonds place an upper limit of <~600 °C (Cody et al. 2008).

Fig. 7 contains a compendium of data constraining the timing of events on the CV parent body and on other early-accreting bodies. Although all the isotopic systems included in this table do not have equivalent precision and accuracy, in aggregate they provide a sufficiently clear timeline to guide the modeling efforts presented in this paper. Specifically, the CV parent body contains chondrules not younger than about 3 Ma after first CAIs. The majority, and perhaps all, CAIs and chondrules in the CV parent body are older than these limits.

Metamorphism of chondrite parent bodies appears to stretch for tens of millions of years, though peak temperatures for the CV parent body were reached at 5 to 10 Ma after CAIs, based on I–Xe chronometry for Allende (Swindle, 1998). These ages are within error of the 5–10 Ma ages Mn/Cr ages for CV fayalites, although no Mn/Cr ages have actually been reported for Allende itself (Nyquist et al., 2009). These chronometric systems are subject to uncertainties associated with the initial abundances of the parent nuclides, their closure temperatures, and the homogeneity of their spatial distribution in the solar system.

These constraints require that the planetesimal have a reasonably thick crust while simultaneously producing a core dynamo. Instantaneous accretion models that consider convective heat transfer produce crusts that are too thin to be stable against eruption and impact foundering, and which have thermal profiles too steep to produce a sufficiently large volume consistent with Allende's constraints. These thin crusts are also too old; younger chondrules in Allende require ongoing accretion.

Planetesimals would be expected to continue accreting mass after the processes proposed here are underway. Thus, colder material with younger chondrules would be added after the majority of the body is accreted, and these younger chondrules would be preferentially placed in near-surface material such as that hypothesized for the Allende source. This initially cold crust will also yield significant metamorphosing but not melting regions consistent with Allende's thermal constraints, over a body still producing a core dynamo (Figs. 2 and 5).

The fraction of ice in the planetesimal also affects the energy required to heat and melt the silicate fraction of the body (Gilmour and Middleton, 2009). Both accretionary and radiogenic heat can be applied to melting (and possibly to evaporating) water before silicate melting begins. Further, accretion of some icy material with the rocky chondritic material would significantly enhance crustal formation through the cooling effect of latent heat of melting. The accretion and differentiation of planetesimals that include both ice and rock is pertinent for not just production of chondrites, but also possibly for production of Pallas and Ceres.

4.3. Densities of solids and liquids and likelihood of eruption

Magma is unlikely to rise through the undifferentiated lid of the planetesimal. Basaltic or picritic magmas would cool and solidify as they rise into the cool crust, limiting their radius of maximum rise. Additionally, buoyancy alone is unlikely to drive silicate eruption in small bodies with cool crusts. Because of the porous nature of unheated chondrites, molten Allende liquids are in many cases denser than the undifferentiated planetesimal lid (Fig. 8). On Earth, Mars, and the Moon, gravity forces buoyant magmas to erupt, while denser magmas may be erupted through volatile pressure. Wilson (1997) predicts fire-fountaining lava eruptions on Vesta driven by volatiles in magmas, but in our models we predict that the magmas will be largely dry. On early-forming planetesimals gradual heating would drive off volatiles before silicate melting begins [this is in contrast to Earth, where volatiles are either introduced to the silicate solids and trigger melting by their presence (Sisson and Grove, 1993) or they exist in equilibrium with near-solidus silicates]. We therefore conclude that only from the hottest bodies with the thinnest crusts will basaltic magmas erupt, or in cases where volatiles were not driven off before magma genesis, will basaltic magmas erupt. The conductive transfer and convection modeled here accounts for the effects of melting from below.

We postulate that the picritic to basaltic silicate magma ocean liquids in the interior magma oceans of these planetesimals will not fully infiltrate and cover the undifferentiated crust of these bodies. Crustal stability in this case relies on three processes: buoyancy of the crust, slow erosion from its bottom, and thickness sufficient to prevent impacts from breaching the crust.

Because of the porous nature of unheated chondrites, molten Allende liquids (red line in Fig. 8) are in many cases denser than the undifferentiated, unsintered, planetesimal lid (grey range in Fig. 8) but close to the density of sintered material. In Fig. 8, the Allende liquid densities are calculated from experimental compositions given in Agee et al. (1995), using partial molar volumes and techniques from Kress and Carmichael (1991) and Lange and Carmichael (1987); also see previous applications of this technique in Elkins-Tanton et al. (2003). All measurements and calculations are done at 1 bar and room temperature. Here, as on the Moon, magmas would require a significant impact basin to erupt onto the surface through the more buoyant crust.

On such a small body viscous traction of the convecting magma ocean liquids on the bottom of the lid will be minimal; not only do magma ocean liquids have low viscosity, but also the small gravitational fields make convective velocities commensurately small.

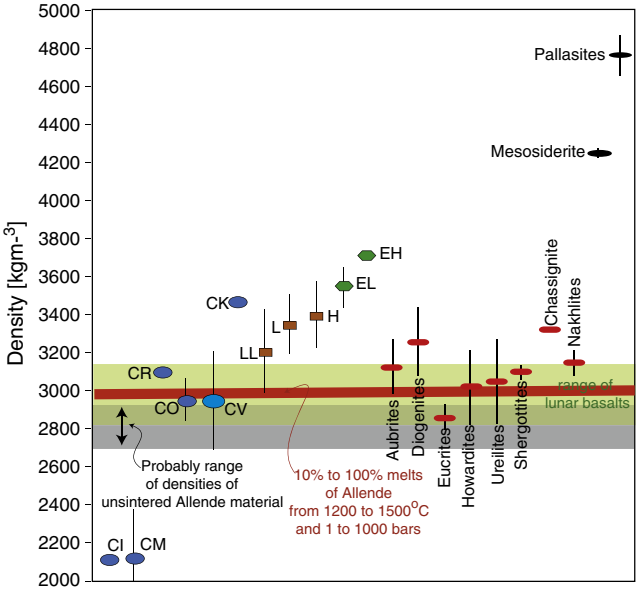

Fig. 8. Densities of materials that would be found in the modeled differentiated planetesimals, and various other solar system materials for comparison. Densities of carbonaceous and ordinary chondrites, achondrites, and iron meteorites from Britt and Consolmagno (2003). Range of lunar basalt densities from Weiczorek et al. (2001). Allende melt densities calculated as described in text.

Erosion of the bottom of the crust through liquid convection is therefore negligible.

Finally, the crust must be thick enough to prevent the majority of impacts from breaching it. The small gravity fields of planetesimals prevent very great impact crater depths. Taylor et al. (1987) estimate that the maximum excavation depth expected on a planetesimal with 500 km diameter is 20 km. Although simple heat transfer in our models produces a thin crust, later accreting material is expected to produce a far thicker crust. We therefore suggest that the average impact will disrupt but not breach the crust and that in most cases impacts will not allow magma to erupt. We conclude that undifferentiated chondritic crusts may successfully persist through the internal magma ocean stage, particularly when the bodies accreted throughout and after the window available for internal heating.

4.4. Source regions for meteorite types in an internally differentiated planetesimal

At temperatures above ~430 °C (Yomogida and Matsui, 1984) the porous chondritic material would sinter into a denser and stronger solid. At about the same temperatures, fluids may be released from the *in situ* chondritic materials. Hydrous, briney, sulfidic, or carbon-rich fluids will be able to rise efficiently through the chondritic crust at Darcy velocities of meters to kilometers per year (Haack et al., 1990; Young et al., 2003). These fluids may to quickly escape into space (Young et al., 2003). Even in the case where a frozen ice crust slows escape, periodic impacts will disrupt this surface and aid escape. Hydrous fluids are therefore not expected to pervasively or homogeneously metasomatize the entire planetesimal crust. We note further that briney fluids are insufficient to create a core dynamo: circulating saltwater of composition like Earth's seawater has electrical conductivity more than four orders of magnitude less than iron-liquid metal [see discussion in Schubert et al. (1996)].

The added cooler material accreting to the top of the crust will experience varying degrees of thermal and fluid metamorphism, depending on its depth and time of accretion. Some late-accreting material will be added after the main pulse of heating and metasomatism, and so will not experience the same intensity of metamorphism. The stochastic nature of crustal additions implies that metamorphic grade and cooling rate may not be correlated in samples from the crust.

These models indicate that dynamos will operate on these bodies for tens of millions of years, allowing a range of accreted crustal conditions to pertain. Only the deepest parts of the crust will be infiltrated by silicate magmas. These events appear to correspond well with the metasomatic and metamorphic events experienced by the CV chondrites, and help to explain why CV chondrites almost never contain fragments of volcanic rock.

The least metamorphosed, brecciated, and reduced CV chondrites containing a solar wind component, such as Vigarano and Mokoia, may have originated nearest the surface. Beneath were the Bali-type oxidized CV chondrites, and at greater depth, the Allende-type oxidized CV chondrites (Fig. 1). Rocks like the metachondrite NWA 3133 may have originated at greatest depth in the undifferentiated crust, while the few higher petrologic-grade clasts found in Mokoia (Krot et al., 1998) may be rare samples of the highly thermally metamorphosed lower crust (Fig. 1). Irons like Bocaiuva (Irving et al., 2004) may have come from the core–mantle boundary region of this same body (Fig. 1). Further, Greenwood et al. (2010) argue that CK and CV chondrites may have formed on the same parent body, with CK chondrites simply being more highly metamorphosed, and therefore, deeper samples.

4.5. The existence of internally differentiated planetesimals today

Because of the limited lifetime of ^{26}Al and the longer apparent period over which chondrite parent bodies were forming, many parent bodies likely heated without significant melting. Bodies that formed before ~1 Ma likely melted sufficiently to produce only a fragile crust, and may have developed into bodies with igneous surfaces like Vesta, while those accreting more slowly would have obtained an internal magma ocean and a thicker, metamorphosed but unmelted crust.

The shapes and masses of the two largest asteroids, 1 Ceres and 2 Pallas, can be consistent with differentiated interiors, conceivably with small iron cores with hydrated silicate or ice–silicate mantles. The range of mantle density permits ice–silicate compositions, though in this scenario for 1 Ceres the mantle is ice-rich (perhaps >50 wt.% if there is no porosity, possibly not compatible with large-scale melting). The corresponding range of mantle density for 2 Pallas permits more silicate-rich compositions than Ceres.

Thus the asteroid melt may contain several examples of early-accreting bodies that are internally differentiated. Unlike Vesta, Ceres and Pallas may retain their primitive crusts over a differentiated interior. This is the central concept of this paper: That early radiogenic of planetesimals can create partially differentiated bodies with undifferentiated crusts, and that these bodies may have experienced magnetic core dynamos, varying degrees of crustal metamorphism or magmatic intrusion, and that some partially differentiated bodies may have persisted to the current day. These bodies likely did not all begin with chondritic composition; Ceres and Pallas, for example, could have very small metallic cores.

5. Conclusions

Planetesimals that largely accreted before ~1.5 Ma after CAIs are likely to differentiate internally through radiogenic heating (Ghosh and McSween, 1998; Hevey and Sanders, 2006; Sahijpal et al., 2007; Urey, 1955). Most of these bodies are capable of producing a core dynamo. The earliest-accreting bodies are likely to obtain igneous crusts through foundering of their thin lids, but bodies that continue to accrete past ~1.5 Ma are likely to have an undifferentiated crust not covered by basalt.

Bodies that are internally differentiated in the manner described here, therefore, may well exist undetected in the asteroid belt. Other asteroids may have lost their hydrostatic shapes through later impacts, and their surfaces may never have been covered with erupted basalt; surfaces of these bodies may have remained chondritic throughout this process. Such surfaces will therefore be composed of irregular, space-weathered primitive material, perhaps with highly altered or even differentiated material at the bottoms of the largest craters and in crater ejecta. This scenario can help explain the mismatch between the enormous diversity (>130) of parent bodies represented by achondrites and the paucity (<10) of basalt-covered asteroids.

Acknowledgements

An NSF Astronomy CAREER grant and the Mitsui Career Development Professorship to L.T.E.-T, a NASA Origins grant and the Victor P. Starr Career Development Professorship to B.P.W., and a NASA/Dawn co-investigator grant to M.T.Z funded this research. The manuscript was improved by reviews by Ian Sanders, Jeff Taylor, and an anonymous reviewer, and by conversations with Hap McSween, David Mittlefehldt, Stein Jacobsen, and Thorsten Kleine.

Appendix A. Supplementary data

Supplementary data to this article can be found online at doi:10.1016/j.epsl.2011.03.010.

References

Agee, C.B., Li, J., Shannon, M.C., Circone, S., 1995. Pressure–temperature phase diagram for the Allende meteorite. J. Geophys. Res. 100, 17725–17740.

Amelin, Y., Krot, A.N., 2007. Pb isotopic age of the Allende chondrules. Meteorit. Planet. Sci. 42, 1321–1335.

Bartels, K.S., Grove, T.L., 1991. High-pressure experiments on magnesian eucrite compositions — constraints on magmatic processes in the eucrite parent body. Proc. Lunar Planet. Sci. Conf. 21, 351–365.

Butler, R.F., 1972. Natural remanent magnetization and thermomagnetic properties of Allende meteorite. Earth Planet. Sci. Lett. 17, 120–128.

Brearley, A., 1997. Disordered biopyriboles, amphibole, and talc in the Allende meteorite: products of nebular or parent body aqueous alteration? Science 276, 1103.

Britt, D.T., Consolmagno, S.J., 2003. Stony meteorite porosities and densitied: a review of the data through 2001. Meteorit. Planet. Sci. 38, 1161–1180.

Carporzen, L., Weiss, B.P., Elkins-Tanton, L.T., Shuster, D.L., Ebel, D.S., Gattacceca, J., 2010. Magnetic evidence for a partially differentiated carbonaceous chondrite parent body. Proc. Natl. Acad. Sci. USA 42, 944.

Carslaw, H.S., Jäger, J.C., 1946. Conduction of Heat in Solids. Oxford University Press, Oxford. 510 pp.

Castillo-Rogez, J., McCord, T.B., 2010. Ceres' evolution and present state constrained by shape data. Icarus 205, 443–459.

Castillo-Rogez, J., Johnson, T.V., Lee, M.H., Turner, N.J., Matson, D.L., Lunine, J., 2009. ^{26}Al decay: heat production and a revised age for Iapetus. Icarus 204, 658–662.

Cody, G.D., Alexander, C.M.O.D., Yabuta, H., Kilcoyne, A.L.D., Araki, T., Ade, H., Dera, P., Fogel, M., Militzer, B., Mysen, B.O., 2008. Organic thermometry for chondritic parent bodies. Earth Planet. Sci. Lett. 272, 446–455.

Connelly, J., Amelin, Y., Krot, A., Bizzarro, M., 2008. Chronology of the solar system's oldest solids. Astrophys. J. Lett. 675, 121–124.

Dermott, S.F., 1979. Shapes and gravitational moments of satellites and asteroids. Icarus 37, 575–586.

Elkins Tanton, L.T., Maroon, E., Krawczynski, M.J., Grove, T.L., 2008. Magma ocean solidification processes on Vesta. Lunar and Planetary Sciences Conference 39, Houston, TX.

Elkins-Tanton, L.T., Parmentier, E.M., Hess, P.C., 2003. Magma ocean fractional crystallization and cumulate overturn in terrestrial planets: implications for Mars. Meteorit. Planet. Sci. 38, 1753–1771.

Fabrichnaya, O.B., 1999. The phase relations in the FeO–MgO–Al_2O_3–SiO_2 system: an assessment of thermodynamic properties and phase equilibria at pressures up to 30 GPa. Calphad 23, 19–67.

Funaki, M., Wasilewski, P., 1999. A relation of magnetization and sulphidation in the parent body of Allende (CV3) carbonaceous chondrite. Meteorit. Planet. Sci. 34, A39.

Ghosh, A., McSween Jr., H.Y., 1998. A thermal model for the differentiation of asteroid 4 Vesta, based on radiogenic heating. Icarus 134, 187–206.

Ghosh, A., McSween Jr., H.Y., 1999. Temperature dependence of specific heat capacity and its effect on asteroid thermal models. Meteorit. Planet. Sci. 34, 121–127.

Ghosh, A., Weidenschilling, S.J., McSween Jr., H.Y., 2003. Importance of the accretion process in asteroid thermal evolution: 6 Hebe as an example. Meteorit. Planet. Sci. 38, 711–724.

Gilmour, J.D., Middleton, C.A., 2009. Anthropic selection of a solar system with a high ^{26}Al/^{27}Al ratio: implications and a possible mechanism. Icarus 201, 821–823.

Gilmour, J.D., Crowther, S.A., Busfield, A., Holland, G., Whitby, J.A., 2009. An early I–Xe age for CB chondrite chondrule formation, and a re-evaluation of the closure age of Shallowater enstatite. Meteorit. Planet. Sci. 44, 573–579.

Greenwood, R.C., Franchi, I.A., Kearsley, A.T., Alard, O., 2010. The relationship between CK and CV chondrites. Geochim. Cosmochim. Acta 74, 1684–1705.

Haack, H., Rasmussen, K.L., Warren, P.H., 1990. Effects of regolith/megaregolith insulation on the cooling histories of differentiated asteroids. J. Geophys. Res. 95, 5111–5124.

Hess, P.C., 1992. Phase equilibria constraints on the formation of ocean floor basalts. In: Morgan, J.P., Blackman, D.K., Sinton, J.M. (Eds.), Mantle Flow and Melt Generation at Mid-Ocean Ridges, American Geophysical Union Monograph, 71, pp. 67–102.

Hevey, P., Sanders, I., 2006. A model for planetesimal meltdown by ^{26}Al and its implications for meteorite parent bodies. Meteorit. Planet. Sci. 41, 95–106.

Hutcheon, I., Marhas, K.K., Krot, A.N., Goswami, J.N., Jones, R.H., 2009. ^{26}Al in plagioclase-rich chnodrules in carbonaceous chondrites: evidence for an extended duration of chondrule formation. Geochim. Cosmochim. Acta 73, 5080–5099.

Irving, A.J., Larson, T.E., Longstaffe, F.J., Rumble, D., Bunch, T.E., Wittke, J.H., Kuehner, S.M., 2004. A primitive achondrite with oxygen isotopic affinities to CV chondrites: implications for differentiation and the size of the CV parent body. EOS Trans. Am. Geophys. Union 85, P31C–PC.

Jacobsen, B., Yin, Q., Moynier, F., Amelin, Y., Krot, A.N., 2008. ^{26}Al,^{26}Mg and ^{207}Pb,^{206}Pb systematics of Allende CAIs: canonical solar initial ^{26}Al/^{27}Al ratio. Earth Planet. Sci. Lett. 272 (1-2), 353–364.

Jeffreys, H., 1959. The Earth. Cambridge University Press, London.

Johansen, A., Oishi, J.S., Mac Low, M.-M., Klahr, H., Henning, T., Youdin, A., 2007. Rapid planetesimal formation in turbulent circumstellar disks. Nature 448, 1022–1025.

Kress, V.C., Carmichael, I.S.E., 1991. The compressibility of silicate liquids containing Fe2O3 and the effect of composition, temperature, oxygen fugacity, and pressure on their redox states. Contrib. Mineralog. Petrol. 108, 82–92.

Krot, A., Scott, E., Zolensky, M., 1995. Mineralogical and chemical modification of components in CV3 chondrites: nebular or asteroidal processing. Meteoritics 30.

Krot, A.N., Petaev, M.I., Scott, E.R.D., Choi, B.G., Zolensky, M.E., Keil, K., 1998. Progressive alteration in CV3 chondrites: more evidence for asteroidal alteration. Meteorit. Planet. Sci. 33, 1065–1085.

Kunihiro, T., Rubin, A., McKeegan, K., Wasson, J., 2004. Initial ^{26}Al/^{27}Al in carbonaceous-chondrite chondrules: too little ^{26}Al to melt asteroids. Geochim. Cosmochim. Acta 68, 2947–2957.

Lange, R.A., Carmichael, I.S.E., 1987. TiO_2–SiO_2 liquids: new measurements and derived partial molar properties. Geochim. Cosmochim. Acta 51, 2931–2946.

Lee, T., Papanastassiou, D.A., Wasserburg, G.J., 1976. Demonstration of ^{25}Mg excess in Allende and evidence for ^{26}Al. Geophys. Res. Lett. 3, 41–44.

Lodders, K., Fegley, B., 1998. The Planetary Scientist's Companion. Oxford University Press, New York.

MacPherson, G.J., Davis, A.M., Zinner, E.K., 1995. The distribution of aluminum-26 in the early solar system: a reappraisal. Meteorit. Planet. Sci. 30, 365–386.

McCoy, T.J., Mittlefehldt, D.W., Wilson, L., 2006. Asteroid differentiation. In: Lauretta, D.S.a.H.Y.M. (Ed.), Meteorites and the Early Solar System II. University of Arizona Press, Tucson, pp. 733–745.

Merk, R., Breuer, D., Spohn, T., 2002. Numerical modeling of ^{26}Al-induced radioactive melting of asteroids considering accretion. Icarus 159, 183–191.

Miyamoto, M., Fujii, N., Takeda, H., 1981. Ordinary chondrite parent body: an internal heating model. Proc. Lunar Planet. Sci. Conf. 12B, 1145–1152.

Monaghan, B.J., Quested, P.N., 2001. Thermal diffusivity of iron at high temperature in both the liquid and solid states. Iron Steel Inst. Jpn. 41, 1524–1528.

Nagata, T., Funaki, M., 1983. Paleointensity of the Allende carbonaceous chondrite. Mem. Natl. Inst. Polar Res. Spec. Issue 30, 403–434.

Nimmo, F., 2009. Energetics of asteroid dynamos and the role of compositional convection. Lunar and Planetary Science Conference XL, p. 1142.

Nyquist, L.E., Kleine, T., Shih, C.-Y., Reese, Y.D., 2009. The distribution of short-lived radioisotopes in the early solar system and the chronology of asteroid accretion, differentiation, and secondary mineralization. Geochim. Cosmochim. Acta 73, 5115–5136.

Opeil, C.P., Consolmagno, G.J., Britt, D.T., 2010. The thermal conductivity of meteorites: new measurements and analysis. Icarus 208, 449–454.

Sahijpal, S., Soni, P., Gupta, G., 2007. Numerical simulations of the differentiation of accreting planetesimals with ^{26}Al and ^{60}Fe as the heat sources. Meteorit. Planet. Sci. 38.

Schmidt, B.E., Thomas, P.C., Bauer, J.M., Li, J.-Y., McFadden, L.A., Mutchler, M.J., Radcliffe, S.C., Rivkin, A.S., Russell, C.T., Parker, J.W., Stern, S.A., 2009. The shape and surface variation of 2 Pallas from the Hubble Space Telescope. Science 9, 275–278.

Schölling, M., Breuer, D., 2009. Numerical simulation of convection in a partially molten planetesimal. European Planetary Science Congress 4, Potsdam, Germany, p. 523.

Schubert, G., Zhang, K., Kivelson, M.G., Anderson, J.D., 1996. The magnetic field and internal structure of Ganymede. Nature 384, 544–545.

Sisson, T.W., Grove, T.L., 1993. Experimental investigations of the role of H_2O in calc-alkaline differentiation and subduction zone magmatism. Contrib. Mineralog. Petrol. 113, 143–166.

Swindle, T., 1998. Implications of I–Xe studies for the timing and location of secondary alteration. Meteorit. Planet. Sci. 33, 1147–1155.

Taylor, G.J., Maggiore, P., Scott, E., Rubin, A., Keil, K., 1987. Original structures, and fragmentation and reassembly histories of asteroids: evidence from meteorites. Icarus 69, 1–13.

Thomas, P., Parker, J., McFadden, L., Russell, C., Stern, S., Sykes, M., Young, E., 2005. Differentiation of the asteroid Ceres as revealed by its shape. Nature 437, 224–226.

Turcotte, D.L., Schubert, G., 2002. Geodynamics. Cambridge University Press, Cambridge. 456 pp.

Urey, H.C., 1955. The cosmic abundances of potassium, uranium, and thorium and the heat balance of the Earth, the Moon, and Mars. Proc. Natl. Acad. Sci. 41, 127–144.

Weiczorek, M.A., Zuber, M.T., Phillips, R.J., 2001. The role of magma buoyancy on the eruption of lunar basalts. Earth Planet. Sci. Lett. 185, 71–83.

Weiss, B.P., Berdahl, J.S., Elkins-Tanton, L., Stanley, S., Lima, E.A., Carporzen, L., 2008. Magnetism on the angrite parent body and the early differentiation of planetesimals. Science 322, 713–716.

Weiss, B.P., Carporzen, L., Elkins-Tanton, L.T., Shuster, D.L., Ebel, D.S., Gattacceca, J., Zuber, M.T., Chen, J.H., Papanastassiou, D.A., Binzel, R.P., Rumble, D., Irving, A.J., 2010. A partially differentiated parent body for CV chondrites. Proc. Lunar Planet. Sci. Conf. 41, 1688.

Wilson, L., Keil, K., 1997. The fate of pyroclasts produced in explosive eruptions on the asteroid 4 Vesta. Meteorit. Planet. Sci. 32, 813–823.

Woolum, D.S., Cassen, P., 1999. Astronomical constraints on nebular temperatures: implications for planetesimal formation. Meteorit. Planet. Sci. 34, 897–907.

Yomogida, K., Matsui, T., 1984. Multiple parent bodies of ordinary chondrites. Earth Planet. Sci. Lett. 68, 34–42.

Young, E., Zhang, K., Schubert, G., 2003. Conditions for pore water convection within carbonaceous chondrite parent bodies: implications for planetesimal size and heat production. Earth Planet. Sci. Lett. 213, 249–259.

Supplementary Data

Chondrites as samples of differentiated planetesimals, *EPSL*

Linda T. Elkins-Tanton, Benjamin P. Weiss and Maria T. Zuber

Calculations included in incremental accretion

As addressed by Merk et al. (2002), Ghosh et al. (2003), and Sahijpal et al. (2007) among others, accretion of these small early bodies is incremental rather than instantaneous. Here, for simplicity, we have based our calculations on instantaneous models, but we find that over the very brief times (0-1.5 Ma after CAI formation) these bodies would be heated radiogenically; heating from the impactors' loss of gravitational potentially energy is unlikely to be of first-order importance (see main text). To make these comparison calculations, we use the equation for impact energy per unit mass

$$E = \frac{h}{2}\left(v_{esc}^2 + v_{rel}^2\right) \qquad \text{(SD 1)}$$

from Melosh (1989), where h is the fraction of total energy that heats the growing planetesimal rather than being radiated into space, v_{esc} is the escape velocity of the growing planetesimal, v_{rel} is the relative velocities between the impactor and the growing body. We further assume, following Weidenschilling et al. (1997) and Ghosh et al. (2003), that the relative velocities of bodies in the accreting nebula are on the order of their escape velocities, and so the two terms can be equated. This final simplification is

$$E = h\frac{2GM}{R}, \qquad \text{(SD 2)}$$

where M and R are the mass and radius of the growing planetesimal, and G is the universal gravitational constant. A conservative value for h is assumed to be 0.5, following Melosh (1989).

We sum the energy calculated in Equation SD2 for a growing planetesimal as its R and M increase from an assumed initial body size to the final planetesimal size. Total accretionary energy is a constant independent of the assumed sizes of impactors, though their individual impacts would create a laterally heterogeneous temperature profile in the growing planetesimal, not treated here. The total heating in these bodies is shown in Fig. SD1.

The incremental accretion models imply that the temperature profiles for these bodies may well be more complex than modelled here. For example, ^{26}Al heating may create a body hottest in the center, surrounded by a cooler shell; additional accretion may heat the surface of the planet, making a locally warm exterior, a radial heat distribution which is nonmonotonic, and a surface heat distribution that is laterally heterogeneous. This implies that CV chondrite constraints may also be consistent with a source region deeper in the parent planetesimal than that implied by our instantaneous accretion model.

SUPPLEMENTARY DATA FIGURE LEGENDS

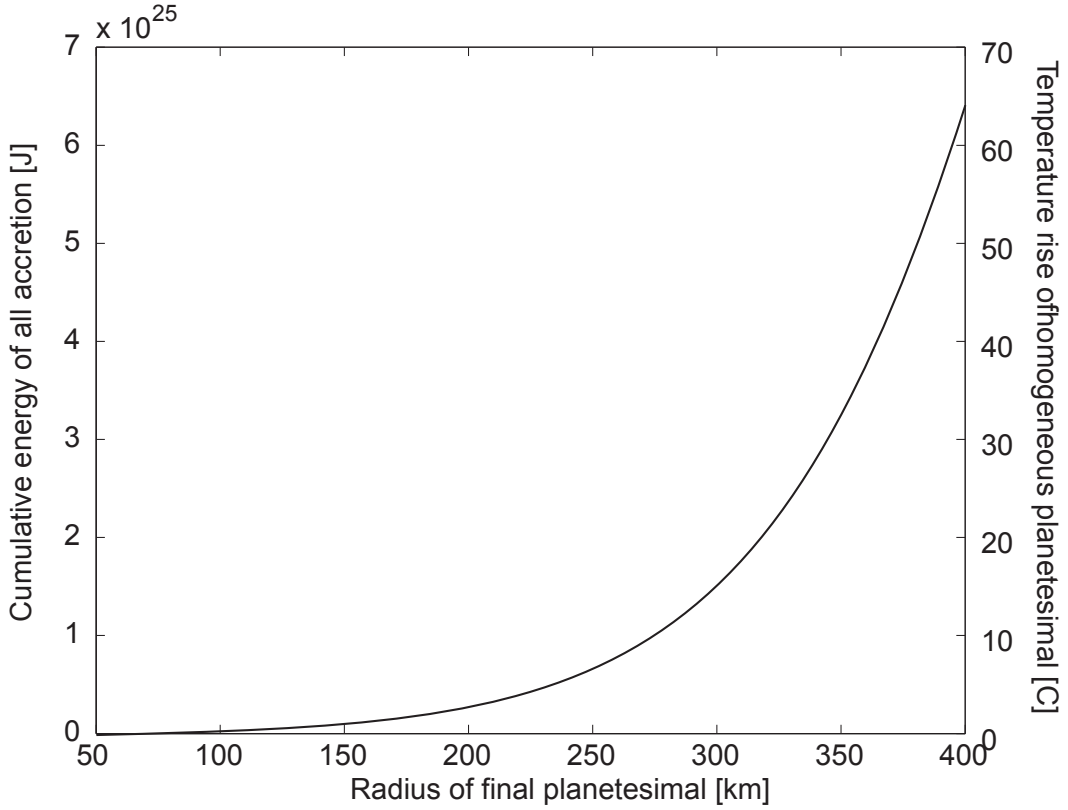

Figure SD 1. Heat of incremental accretion for varying final planetesimal sizes calculated from Equation SD4. Heating is relatively insignificant compared to radiogenic heating in the first 1.5 Ma after CAIs.

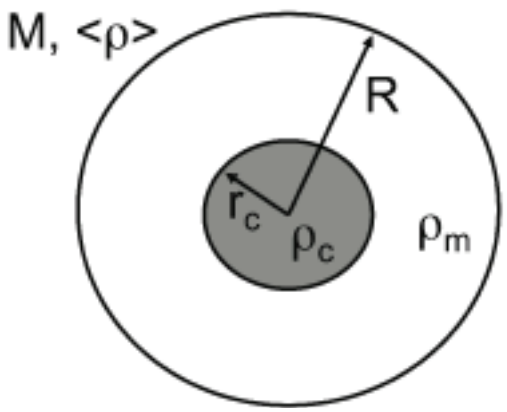

Figure SD 2. Schematic of internal structure of a planetary body composed of a core and mantle. Variables are defined in the text.

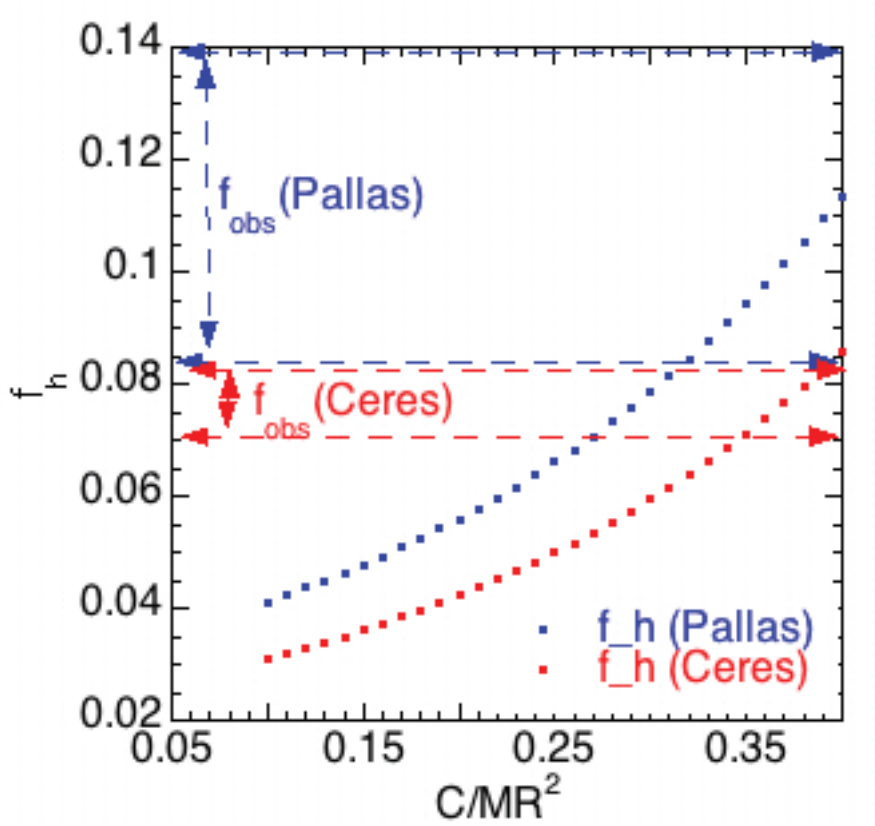

Figure SD 3. Dots represent model of equilibrium shape for Ceres and Pallas as a function of C/Ma^2 for Ceres and Pallas based on Equation (SD7). Dashes represent range of observed flattening $f = (a\text{-}c)/a$ based on Table 2.

SUPPLEMENTARY DATA TABLES

Table SD1: Ages of early solar system materials and processes used in Fig. SD6.

Category	Minus error	Age	Plus error	System	Tied to CAI? *	Meteorite or material being dated, or Notes	Ref.
CAIs	0.4	4569.5	0.4	Pb-Pb		CV Efremovka CAIs	(Baker et al., 2005)
	0.5	4568.5	0.5	U-Pb		CAIs plus chondrules	(Bouvier et al., 2007)
	0.7	4568.3	0.7	Hf-W		Allende CAIs	(Burkhardt et al., 2008)
	9.4	4568.1	9.4	Pb-Pb		Allende CAIs	(Bouvier et al., 2007)
	0.93	4567.72	0.93	Pb-Pb		Allende CAIs	(Connelly et al., 2008)
	0.36	4567.6	0.36	U-Pb		Allende CAIs	(Jacobsen et al., 2008)
	0.6	4567.2	0.6	Pb-Pb		CV Efremovka CAIs	(Amelin, 2002)
	0.81	4565.32	0.81	U-Pb		Allende	(Connelly and Bizzarro, 2008)
				Al-Mg		"Allende CAIs formed over a period as short as 50,000 years"	(Bizzarro et al., 2004)
Iron meteorites	1.7	4569.12	1.6	Hf-W	yes	IIIAB Henbury	(Scherstén et al., 2006)
	3	4568.72	3	Hf-W	yes	IIIF	(Burkhardt et al., 2008)
	2	4568.52	1.6	Hf-W	yes	IVA Duchesne	(Scherstén et al., 2006)
	1.5	4568.22	1.7	Hf-W	yes	IIAB El Burro	(Scherstén et al., 2006)
	1.8	4567.72	1.7	Hf-W	yes	IVA Bristol	(Scherstén et al., 2006)
	1.6	4567.62	1.8	Hf-W	yes	IIAB Coahuila A	(Scherstén et al., 2006)
	2	4567.02	2	Hf-W	yes	IIAB	(Burkhardt et al., 2008)
	2	4566.97	2	Hf-W	yes	Average IIAB	(Kleine et al., 2005)
	1.5	4566.92	1.5	Hf-W	yes	IIIAB	(Burkhardt et al., 2008)
	1.6	4566.92	1.8	Hf-W	yes	IVB Cape of Good Hope	(Scherstén et al., 2006)
	1.5	4566.82	1.5	Hf-W	yes	IVA	(Burkhardt et al., 2008)
	1.6	4566.72	1.6	Hf-W	yes	IIIE	(Burkhardt et al., 2008)
	1.7	4566.32	1.9	Hf-W	yes	IIIAB Canyon	(Scherstén et al., 2006)
	1.7	4566.22	2	Hf-W	yes	IAB-IIICD Toluca	(Scherstén et al., 2006)
	1.9	4566.02	2	Hf-W	yes	IIIF Moonbi	(Scherstén et al., 2006)
	1.5	4565.72	1.5	Hf-W	yes	IVB	(Burkhardt et al., 2008)
	2.5	4565.72	2.5	Hf-W	yes	IC	(Burkhardt et al., 2008)
	2	4563.72	2.4	Hf-W	yes	IAB-IIICD Coolac	(Scherstén et al., 2006)
Chondrules	0.2	4567.02	0.2	Al-Mg	yes	LL3 Bishunpur	(Mostefaoui et al., 2002)
	0.4	4565.32	0.7	Al-Mg	yes	LL3 Bishunpur	(Mostefaoui et al.,

							2002)
	1	4566.6	1	Pb-Pb		Chondrules in CV3 Allende	(Amelin and Krot, 2007)
	0.6	4566.12	1.2	Al-Mg	yes	C2-ung Acfer 094	(Sugiura and Krot, 2007)
	0.3	4565.52	0.4	Al-Mg	yes	C2-ung Acfer 094	(Sugiura and Krot, 2007)
	0.7	4566.02	0.7	Hf-W	yes	Chondrules in H chondrites	(Kleine et al., 2008b)
	0.4	4565.62	0.4	Al-Mg	yes	Type I chondrules in CO3 Yamato 81020	(Kurahashi et al., 2008)
	0.35	4565.47	0.35	Al-Mg	yes	Al-rich chondrules in CO3 Yamato 81020	(Kurahashi et al., 2008)
	0.45	4565.45	0.45	Pb-Pb		CV3 Allende	(Connelly et al., 2008)
	0.5	4565.22	0.5	Al-Mg	yes	Type II chondrules in CO3 Yamato 81020	(Kurahashi et al., 2008)
	0.6	4564.7	0.6	Pb-Pb		CR2 Acfer 059	(Amelin, 2002)
	0.9	4562.8	0.9	Pb-Pb		CBb Hammadah al Hamra 237	(Krot et al., 2005)
	0.5	4562.7	0.5	Pb-Pb		CBa Gujba	(Krot et al., 2005)
Chondrite parent bodies	0.7	4566.02	0.7	Hf-W	yes	H4 Ste. Margeurite	(Kleine et al., 2008b)
	1.2	4565.8	1.2	Al-Mg		H4 Ste. Margeurite and H4 Forest Vale parent body accretion	(Gounelle and Russell, 2005)
	1	4563	1	Pb-Pb		H4 Ste. Marguerite phosphate	(Trieloff et al., 2003)
	0.7	4562.7	0.7	Pb-Pb		H4 Ste. Marguerite phosphate	(Göpel et al., 1994)
	0.8	4561.82	0.8	Hf-W	yes	H5 Richartdton and ALH84069	(Kleine et al., 2008b)
	1	4561	1	Pb-Pb		H4 Forest Vale phosphate	(Trieloff et al., 2003)
	0.7	4560.9	0.7	Pb-Pb		H4 Forest Vale phosphate	(Göpel et al., 1994)
	0.9	4558.12	0.9	Hf-W	yes	H6 Kernouve and Estacado	(Kleine et al., 2008b)
	1	4556	1	Pb-Pb		H5 Sena phosphate	(Trieloff et al., 2003)
	3	4556	3	Pb-Pb		H5 Nadiobondi phosphate	(Trieloff et al., 2003)
	3.4	4555.6	3.4	Pb-Pb		H5 Nadiabondi phosphate	(Göpel et al., 1994)
	0.6	4551.4	0.6	Pb-Pb		H5 Richardton phosphate	(Göpel et al., 1994)
	1	4551	1	Pb-Pb		H5 Richardton phosphate	(Trieloff et al., 2003)
	0.7	4550.2	0.7	Pb-Pb		H5 Allegan phosphate	(Göpel et al., 1994)
	1	4550	1	Pb-Pb		H5 Allegan phosphate	(Trieloff et al., 2003)
Notes				Al-Mg		Allende chondrules began forming at the same time as CAIs and continued for at least 3 M yr	(Bizzarro et al., 2004; Hutcheon et al., 2009)
				Pb-Pb		Ste. Margeurite parent body cooled from 830 to 530ºC between 4,565 and 4,563 Ma	(Bouvier et al., 2007)
				Pb-Pb		Nadiabondi cooled over the	(Bouvier et al., 2007)

						same temperature range from 4,559 to 4,556 Ma	
						Aqueous alteration occurred on the Allende parent body as late as 7 - 17 Ma after CAIs	(Hutcheon et al., 1998)
				Mn-Cr			
				I-Xe		Allende sodalite formed 5 Ma after first CAIs	(Swindle, 1998)
				I-Xe		Allende sodalite minerals were at 300 to 500C at 10 Ma after first CAIs	(Swindle, 1998)
Acapulcoite -Lodranites	1.4	4561.3	1.4	Hf-W	yes	NWA 2627, NWA 2775, Dhofar 125	(Touboul et al., 2007)
Angrites	0.1	4566.2	0.1	Pb-Pb		Sahara 99555, NWA1296	(Baker et al., 2005)
	0.38	4564.86	0.38	U-Pb		Sahara 99555 pyroxenes	(Amelin, 2008)
	0.12	4564.42	0.12	U-Pb		d'Orbigny pyroxene	(Amelin, 2008)
	0.6	4563.9	0.6	Pb-Pb		d'Orbigny	(Zartman et al., 2006)
	1.1	4563.42	1.1	Al-Mg	yes	d'Orbigny	(Gounelle and Russell, 2005)
	1.3	4562.4	1.3	Hf-W	yes	d'Orbigny	(Markowski et al., 2007)
	1.6	4562.4	1.6	Pb-Pb		Asuka 881371	(Zartman et al., 2006)
	1.3	4562.0	1.3	Hf-W	yes	Sahara 99555	(Markowski et al., 2007)
	0.6	4559.62	0.6	Hf-W	yes	NWA 4590	(Kleine et al., 2008a)
	0.8	4558.72	0.8	Hf-W	yes	NWA 4801	(Kleine et al., 2008a)
	0.18	4558.62	0.18	U-Pb		LEW 86010 pyroxenes	(Amelin, 2008)
	0.15	4558.55	0.15	U-Pb		LEW 86010 pyroxene	(Amelin, 2008)
	0.13	4557.65	0.13	U-Pb		Angra dos Reis pyroxene	(Amelin, 2008)
	3.3	4557.6	3.3	Hf-W	yes	NWA 2999	(Markowski et al., 2007)
eucrite	1	4564.92	1	Al-Mg	yes	Asuka 881394	(Gounelle and Russell, 2005)
	2.2	4564.72	2.2	Hf-W	yes	Eucrites	(Kleine et al., 2004)
	1.4	4563.72	1.4	Hf-W	yes	Vesta differentiation	(Kleine et al., 2004)
Mars	5	4555.2	5	Hf-W	yes	SNC meteorites	(Kleine et al., 2004)

Ages marked “Tied to CAI” are calculated relative to the assumed age of initial condensation in the nebula, here the first CAIs from Allende as reported in Connelly et al. (2008): 4,567.72 Ma.

Table SD2: Parameters for 1 Ceres and 2 Pallas

Parameter	1 Ceres	Ref.	2 Pallas	Ref.
M, kg	$(9.35 \pm 0.056) \times 10^{20}$	(Konopliv et al., 2006)	$(2.04 \pm 0.056) \times 10^{20}$	(Konopliv et al., 2006)
R, km	476.2 ± 1.7	(Thomas et al., 2005)	278 ± 9	(Konopliv et al., 2006)
a, km	487.3 ± 1.8	(Thomas et al., 2005)	291 ± 9	(Konopliv et al., 2006)
c, km	454.0 ± 4.5	(Thomas et al., 2005)	250 ± 9	(Konopliv et al., 2006)
$\langle\rho\rangle$ kg m^{-3}	2077 ± 36	(Jeffreys, 1959)	2400 ± 250	(Konopliv et al., 2006)
ω, rad s^{-1}	1.923×10^{-4}	(Jeffreys, 1959)	2.234×10^{-4}	(Konopliv et al., 2006)

References

Amelin, Y., 2002. Lead Isotopic Ages of Chondrules and Calcium-Aluminum-Rich Inclusions. Science 297, 1678-1683.

Amelin, Y., 2008. U-Pb ages of angrites. Geochimica Et Cosmochimica Acta 72, 221-232.

Amelin, Y., Krot, A.N., 2007. Pb isotopic age of the Allende chondrules. Meteoritics and Planetary Science 42, 1321-1335.

Baker, J., Bizzarro, M., Wittig, N., Connelly, J., Haack, H., 2005. Early planetesimal melting from an age of 4.5662 Gyr for differentiated meteorites. Nature 436, 1127-1131.

Bizzarro, M., Baker, J., Haack, H., 2004. Mg isotope evidence for contemporaneous formation of chondrules and refractory inclusions. Nature 431, 275-278.

Bouvier, A., Blichert-Toft, J., Moynier, F., Vervoort, J., Albarède, F., 2007. Pb-Pb dating constraints on the accretion and cooling history of chondrites. Geochimica Et Cosmochimica Acta 71, 1583-1604.

Burkhardt, C., Kleine, T., Bourdon, B., Palme, H., Zipfel, J., Friedrich, J.M., Ebel, D.S., 2008. Hf-W mineral isochron for Ca,Al-rich inclusions: Age of the solar system and the timing of core formation in planetesimals. Geochimica Et Cosmochimica Acta 72, 6177-6197.

Connelly, J., Amelin, Y., Krot, A., Bizzarro, M., 2008. Chronology of the Solar System's Oldest Solids. The Astrophysical Journal Letters 675, 121-124.

Connelly, J., Bizzarro, M., 2008. Pb,Pb dating of chondrules from CV chondrites by progressive dissolution. Chemical Geology, 1-9.

Ghosh, A., Weidenschilling, S.J., McSween Jr., H.Y., 2003. Importance of the accretion process in asteroid thermal evolution: 6 Hebe as an example. Meteoritics and Planetary Science 38, 711-724.

Göpel, C., Manhès, G., Allègre, C., 1994. U-Pb systematics of phosphates from equilibrated ordinary chondrites. Earth and Planetary Science Letters 121, 153-171.

Gounelle, M., Russell, S.S., 2005. On early Solar System chronology: Implications of an heterogeneous spatial distribution of 26Al and 53Mn. Geochimica et Cosmochimica Acta 69, 3129-3144.

Hutcheon, I., Krot, A., Keil, K., Phinney, D., Scott, E., 1998. 53Mn-53Cr dating of fayalite formation in the CV3 chondrite Mokoia: evidence for asteroidal alteration. Science 282, 1865.

Hutcheon, I., Marhas, K.K., Krot, A.N., Goswami, J.N., Jones, R.H., 2009. ^{26}Al in plagioclase-rich chnodrules in carbonaceous chondrites: Evidence for an extended duration of chondrule formation. Geochimica Et Cosmochimica Acta 73, 5080-5099.

Jacobsen, B., Yin, Q., Moynier, F., Amelin, Y., Krot, A.N., 2008. ^{26}Al,^{26}Mg and ^{207}Pb,^{206}Pb systematics of Allende CAIs: Canonical solar initial ^{26}Al/^{27}Al ratio. Earth and Planetary Science Letters.

Jeffreys, H., 1959. The Earth, 4th ed. Cambridge University Press, London.

Kleine, T., Bourdon, B., Burkhardt, C., Irving, A.J., 2008a. Hf-W chronometry of angrites: Constraints on the absolute age of CAIs and planetesimal accretion times, The Lunar and Planetary Science Conference. The Lunar and Planetary Institute, Houston, TX, p. 2367.

Kleine, T., Mezger, K., Munker, C., Palme, H., Bischoff, A., 2004. ^{182}Hf-^{182}W isotope systematics of chondrites, eucrites, and martian meteorites: Chronology of core formation and early mantle differentiation in Vesta and Mars. Geochimica Et Cosmochimica Acta 68, 2935-2946.

Kleine, T., Mezger, K., Palme, H., Scherer, E., Münker, C., 2005. Early core formation in asteroids and late accretion of chondrite parent bodies: Evidence from 182Hf-182W in CAIs, metal-rich chondrites, and iron meteorites. Geochimica et Cosmochimica Acta 69, 5805-5818.

Kleine, T., Touboul, M., Van Orman, J., Bourdon, B., Maden, C., Mezger, K., Halliday, A., 2008b. Hf-W thermochronometry: Closure temperature and constraints on the accretion and cooling history of the H chondrite parent body. Earth and Planetary Science Letters 270, 106-118.

Konopliv, A.S., Yoder, C.F., Standish, E.M., Yuan, D.-N., Sjogren, W.L., 2006. A global solution for the Mars static and seasonal gravity, Mars orientation, Phobos and Deimos masses, and Mars ephemeris. Icarus 182, 23-50.

Krot, A., Amelin, Y., Cassen, P., Meibom, A., 2005. Young chondrules in CB chondrites from a giant impact in the early Solar System. Nature 436, 989-992.

Kurahashi, E., Kita, N.T., Nagahara, H., Morishita, Y., 2008. ^{26}Al,^{26}Mg systematics of chondrules in a primitive CO chondrite. Geochimica et Cosmochimica Acta 72, 3865-3882.

Markowski, A., Quitté, G., Kleine, T., Halliday, A., Bizzarro, M., Irving, A., 2007. Hafnium-tungsten chronometry of angrites and the earliest evolution of planetary objects. Earth and Planetary Science Letters 262, 214-229.

Melosh, H.J., 1989. Impact Cratering. Oxford University Press, New York.

Merk, R., 2002. Numerical Modeling of ^{26}Al-Induced Radioactive Melting of Asteroids Considering Accretion. Icarus 159, 183-191.

Mostefaoui, S., Kita, N.T., Togashi, S., Tachibana, S., Nagahara, H., Morishita, Y., 2002. The relative formation ages of ferromagnesian chondrules inferred from their initial aluminum-26/aluminum-27 ratios. Meteoritics and Planetary Science 37, 421-438.

Sahijpal, S., Soni, P., Gupta, G., 2007. Numerical simulations of the differentiation of accreting planetesimals with ^{26}Al and ^{60}Fe as the heat sources. Meteoritics &# 38; Planetary Science.

Scherstén, A., Elliott, T., Hawkesworth, C., Russell, S., Masarik, J., 2006. Hf,W evidence for rapid differentiation of iron meteorite parent bodies. Earth and Planetary Science Letters 241, 530-542.

Sugiura, N., Krot, A.N., 2007. ^{26}Al-^{26}Mg systematics of Ca-Al-rich inclusions, amoeboid olivine aggregates, and chondrules from the ungrouped carbonaceous chondrite Acfer 094. Meteoritics and Planetary Science 42, 1183-1195.

Swindle, T., 1998. Implications of I-Xe studies for the timing and location of secondary alteration. Meteoritics & Planetary Science 33, 1147-1155.

Thomas, P.C., Parker, J.W., McFadden, L.A., Russell, C.T., Stern, S.A., Sykes, M.V., Young, E.F., 2005. Differentiation of the asteroid Ceres as revealed by its shape. Nature 437, 224-226.

Touboul, M., Kleine, T., Bourdon, B., Irving, A.J., Zipfel, J., 2007. Hf-W evidence for rapid accretion and fast cooling of the Acapulcoite parent body, Lunar and Planetary Science Conference. The Lunar and Planetary Institute, Houston, TX, p. 2317.

Trieloff, M., Jessberger, E., Herrwerth, I., Hopp, J., Fiéni, C., Ghélis, M., Bourot-Denise, M., Pellas, P., 2003. Structure and thermal history of the H-chondrite parent asteroid revealed by thermochronometry. Nature 422, 502-506.

Weidenschilling, S.J., Spaute, D., Davis, D.R., Marzari, F., Ohtsuki, K., 1997. Accretional evolution of a planetesimal swarm. Icarus 128, 429-455.

Zartman, R.E., Jagoutz, E., Bowring, S.A., 2006. Pb-Pb dating of the d'Orbigny and Asuka 881371 angrites and a second absolute time calibration of the Mn-Cr chronometer, The Lunar and Planetary Science Conference. The Lunar and Planetary Institute, Houston, TX, p. 1580.